

Polarized field saturation spectroscopy

Murray Sargent III*

*Institut für Theoretische Physik der Universität Stuttgart
and Max-Planck-Institut für Festkörperforschung, Stuttgart, Germany*

(Received 24 November 1975)

A new kind of saturation spectroscopy is discussed in which the direction and polarization of a nonsaturating probe wave is varied with respect to that of a saturating wave. Angular momenta, Landé g values, and atomic lifetimes are obtained with greater ease than with earlier Zeeman laser methods. In particular, the theory is dramatically simplified.

Traditional absorption and emission spectroscopies have given a great deal of information about the structure of matter and the interaction of radiation with matter. However, often too many transitions come into play, e.g., through inhomogeneous broadening or band structure, thereby preventing one from measuring quantities such as homogeneously broadened and level lifetimes. Saturation spectroscopy,¹ a field made possible by the advent of the laser, allows one to study transitions even under an inhomogeneously broadened envelope or to study selected interband transitions in a semiconductor.² Specifically, a strong laser beam is used to saturate an electric dipole transition, while the absorption of a weak (generally nonsaturating) probe beam is studied as a function of probe frequency. This kind of technique has produced the highest-resolution spectra to date,³ highest by several orders of magnitude.

So far little attention has been paid to the relative polarizations of the two waves.⁴ In this comment, we show how the relative polarizations not only influence the results of saturation spectroscopy, but in fact can be used to measure information often not easily obtained with traditional methods, owing, for example, to the presence of inhomogeneous broadening.

The fundamental physics involved is well known in the Zeeman laser field,⁵ but there the various constants (J and g values, lifetimes) have been typically measured on samples placed inside the laser cavity operating near or on a laser transition of interest.⁶⁻⁹ This configuration allows saturation to be achieved easily, but complicates the corresponding theory substantially (if not hopelessly) by introducing standing waves, by having both "probe" and saturating waves saturate, and by having the sample enter into the laser equations of motion. Here we describe corresponding experiments outside the cavity, avoiding these limitations and allowing J , g and lifetime measurements on any saturable transition in spite of inhomogeneous broadening. The emphasis is

on J values, for which the approach is particularly simple, but discussion of g values and lifetimes is also given.

Using analysis given in Refs. 10 and 11, one studies the absorption of a probe by a medium subjected to a saturating wave of either identical or orthogonal polarization to that of the probe. For identical polarizations, both probe and saturating waves involve the same combinations of transitions and matrix elements, while for orthogonal polarizations they involve different combinations. It will be shown here that an appropriate combination of transmitted probe intensities [Eq. (4)] depends only on the J values of the levels.¹² For the orthogonal polarization case, both probe and saturating waves are chosen to travel in the same direction and hence are called co-running. They can be distinguished through the use of polarizers [see Fig. 1(a)] or by a slight angle between their directions of propagation, as shown in Fig. 1(c). For the same polarization case and a Doppler-broadened medium, the waves can be taken to travel in opposite directions (counter running), thereby allowing the two waves to be distinguished [see Fig. 1(b)] and causing the coherent interaction (saturation grating) induced in the medium to be reduced by the Doppler broadening.¹³ For the stationary-atom case, this grating term doubles the saturation for the counter-running case. For any medium, the same polarization case can be performed in the co-running configuration of Fig. 1c provided that the cross-saturation coefficient θ_{\parallel} in the following is doubled. Other combinations and directions can be used, but then the difference between the upper- and lower-level decay constants may influence the result. Both linearly and circularly polarized wave combinations are considered in the present work.

To describe the interactions, we introduce the following intensities: I_s , the saturating wave intensity; I_{p0} , the initial probe intensity; and the three transmitted probe intensities I_{pu} , $I_{p\parallel}$, and

$I_{p\perp}$ for $I_s = 0$, I_s with the same polarization as I_{p0} , and I_s with the orthogonal polarization, respectively. The unsaturated transmitted probe intensity is given by Beer's law as

$$I_{pu} = I_{p0} e^{-\alpha_0 L} \cong I_{p0}(1 - \alpha_0 L), \quad (1)$$

where L is the sample length and α_0 is the linear absorption coefficient. In the presence of saturating waves of equal or orthogonal polarizations, α_0 is reduced to the values α_{\parallel} and α_{\perp} , respectively, that is,

$$I_{p\parallel} \cong I_{p0}(1 - \alpha_{\parallel} L), \quad I_{p\perp} \cong I_{p0}(1 - \alpha_{\perp} L). \quad (2)$$

According to third-order perturbation theory,¹⁰ the saturated absorption coefficients are given by

$$\alpha_{\parallel} = \alpha_0 - \theta_{\parallel} I_s, \quad \alpha_{\perp} = \alpha_0 - \theta_{\perp} I_s, \quad (3)$$

where θ_{\parallel} and θ_{\perp} are cross-saturation coefficients. Combining (1)–(3), we find

$$(I_{p\perp} - I_{pu}) / (I_{p\parallel} - I_{pu}) = \theta_{\perp} / \theta_{\parallel}. \quad (4)$$

From Ref. 10, we find that this ratio is given for centrally tuned circular polarizations by

$$\frac{\theta_{\perp}}{\theta_{\parallel}} = \left[\sum_{a'} \sum_{b'} \delta_{a', b'+1} |\varphi_{a', b'}|^2 (|\varphi_{a', -2, b'}|^2 + |\varphi_{a', b'+2}|^2) \right] / \sum_{a'} \sum_{b'} \delta_{a', b'+1} |\varphi_{a', b'}|^4, \quad (5)$$

where a' and b' index magnetic sublevels of the upper (a) and lower (b) levels of the transition and $\varphi_{a', b'}$ is the electric-dipole matrix element between those levels, given by (12-23) of Ref. 5. According to Eqs. (12-45)–(12-47) of Ref. 5 this has the explicit value

$$\frac{\theta_{\perp}}{\theta_{\parallel}} = \begin{cases} (2J+3)(2J-1)/(2J^2+2J+1), & J \rightarrow J, \text{ circular,} \\ (2J^2+4J+5)/(6J^2+12J+5), & J \rightarrow J+1, \text{ circular.} \end{cases} \quad (6a)$$

$$\theta_{\parallel} = \begin{cases} (2J+3)(2J-1)/(2J^2+2J+1), & J \rightarrow J, \text{ circular,} \\ (2J^2+4J+5)/(6J^2+12J+5), & J \rightarrow J+1, \text{ circular.} \end{cases} \quad (6b)$$

In the limit of large J , these go to 2 for $J \rightarrow J$ and to $\frac{1}{3}$ for $J \rightarrow J+1$.

Similarly one finds for centrally tuned linear polarizations the ratio

$$\frac{\theta_{\perp}}{\theta_{\parallel}} = \left[\sum_{a'} \sum_{b'} \delta_{a', b'} |\varphi_{a', b'}|^2 \sum_{\pm} (|\varphi_{a', \pm 1, b'}|^2 + |\varphi_{a', b' \pm 1}|^2) \right] / \sum_{a'} \sum_{b'} \delta_{a', b'} |\varphi_{a', b'}|^4, \quad (7)$$

which, with Eqs. (12-23) and (F-43) of Ref. 5, and algebra, reduces to

$$\frac{\theta_{\perp}}{\theta_{\parallel}} = \begin{cases} (2J^2+2J+1)/(3J^2+3J-1), & J \rightarrow J, \text{ linear,} \\ (6J^2+12J+5)/(4J^2+8J+5), & J \rightarrow J+1, \text{ linear.} \end{cases} \quad (6c)$$

$$\theta_{\parallel} = \begin{cases} (2J^2+2J+1)/(3J^2+3J-1), & J \rightarrow J, \text{ linear,} \\ (6J^2+12J+5)/(4J^2+8J+5), & J \rightarrow J+1, \text{ linear.} \end{cases} \quad (6d)$$

Here the limiting values for large J are $\frac{2}{3}$ for $J \rightarrow J$ and $\frac{3}{2}$ for $J \rightarrow J+1$. The four combinations are plotted as a function of J in Fig. 2.

We see that the method gives good general discrimination for low- J values, and for high- J values it is easy to distinguish between $J \rightarrow J$ and $J \rightarrow J+1$ types of transitions. From Dienes's theory¹¹ one can show that an increase in I_s to the saturation intensity value (population difference equal to one-half of its linear difference) causes the various ratios to approach unity by about 7% (for homogeneous broadening).

The question naturally arises as to what is happening physically. A partial answer is as follows: For the $J=1 \rightarrow 0$ or $1 \rightarrow -1$ cases, the four ratios in (6) are all unity. In the circular-polarization cases (6a) and (6b), the matrix elements for both equal and orthogonal polarizations are all the same. For the linear-polarization cases (6c) and (6d) the matrix element squares $|\varphi_{a', \pm 1, b'}|^2$ in (7) entering θ_{\perp} have the value of the $|\varphi_{a', b'}|^2$, but

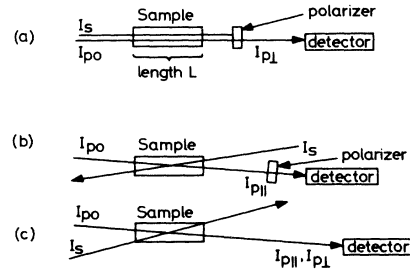


FIG. 1. Diagram of proposed measurement setups. (a) Measurement of transmitted probe intensity $I_{p\perp}$ in the presence of an orthogonally polarized saturating wave. (b) Measurement of transmitted probe intensity $I_{p\parallel}$ in the presence of a saturation wave with the same polarization. Polarizer is included in (b) to help equalize linear transmissions in cases (a) and (b). (c) Alternative configuration to measure both $I_{p\perp}$ and $I_{p\parallel}$, in which the saturation predicted by $I_{p\parallel}$ is twice as great as that in (b) (because of the contribution of the "population-pulsation" term reduced in the counter-running configuration by Doppler broadening). A third measurement is performed with $I_s = 0$, giving the unsaturated transmitted probe intensity I_{pu} .

occur twice as often. For the case of large J values, we consider circular polarizations first. For $J \rightarrow J+1$, $J > 0$, the matrix elements $\varphi_{a'b'}$ = $\varphi_{J,J+1}$ in (5) have the largest magnitudes. The parallel coefficient θ_{\parallel} has this large value to the fourth power, while the θ_{\perp} obtains it only to the second power. Hence $\theta_{\perp}/\theta_{\parallel} < 1$. Conversely, for $J \rightarrow J$, $J > 0$, the large matrix elements are in the middle ($\varphi_{a'b'} = \varphi_{0,1}$ has the largest magnitude). On the average the cross-saturation coefficient θ_{\perp} gets more of these large values than the θ_{\parallel} , thereby causing the ratio (6) to exceed unity.

For the linear polarizations, we have to consider $\varphi_{a'b'}$ in (7) for $a' = b'$ as well as for $a' = b' \pm 1$. For $J \rightarrow J+1$, $J > 0$, the largest matrix elements are the $\varphi_{J,J+1}$ and $\varphi_{0,0}$. The θ_{\parallel} gets $\varphi_{0,0}$ to the fourth power. θ_{\perp} never does quite as well on a single combination, but has twice as many contributions, thereby yielding $\theta_{\perp}/\theta_{\parallel} > 1$, just the opposite of the corresponding circular-polarization case. For $J \rightarrow J$, the matrix elements $\varphi_{a',b'=a'}$ = $\varphi_{a'a'}$, thus weighting the outermost φ_{JJ} heavily and giving θ_{\parallel} the advantage. Hence for this case $\theta_{\perp}/\theta_{\parallel} < 1$, also the opposite of the corresponding circular-polarization case.

This discussion shows how the various matrix elements enter the cross-saturation coefficients. A complete physical explanation would include an interpretation revealing why the Clebsch-Gordan coefficients have the values they have, but this is beyond the scope of this work.

Although the emphasis in this communication is on J values, the method can be readily extended to study g values and level lifetimes by using magnetic fields and a frequency difference between the saturating and probe waves. The theory is considerably simpler than for the corresponding work⁶⁻⁹ within the laser cavity. Specifically, the linearity of the probe should allow theories of arbitrarily large saturation intensities to be written. A particular example is given by the resonance (following from the theory of Ref. 10) that occurs when the frequency difference between probe and saturating waves equals the Zeeman splitting. This allows the g values to be measured. The corresponding work of Refs. 6-9 within the cavity of a multimode laser must be treated with a substantially more complicated theory, which is nevertheless limited to small intensities (pertur-

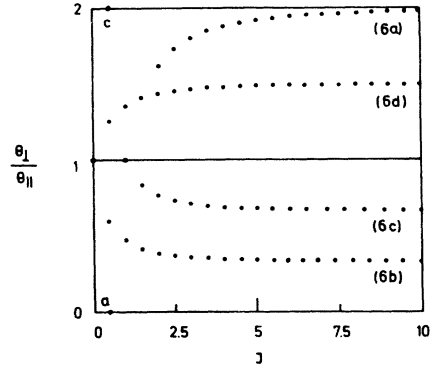


FIG. 2. Graphs of the cross-saturation ratios $\theta_{\perp}/\theta_{\parallel}$ given by Eq. (6). (6a) gives the $J \rightarrow J$, circular-polarization case, (6b) $J \rightarrow J+1$, circular, (6c) $J \rightarrow J$, linear, and (6d) $J \rightarrow J+1$, linear. Two points for $J = \frac{1}{2}$ are labeled specially (one at the value 2 and one at zero), since it is not otherwise obvious to which ratio they belong. The $J = 1 \rightarrow 0$ and $1 \rightarrow 1$ cases all have the value unity. The limiting value for large J are 2, $\frac{1}{3}$, $\frac{2}{3}$, and $\frac{3}{2}$ for (6a)–(6d), respectively.

bation theory). The principal advantage of putting the sample cell inside the laser cavity is that it may be easier to obtain saturation. But this advantage is becoming less and less important as higher-power tunable lasers are developed. In related work, Gorlicki and Dumont¹⁴ have observed the magnetic tuning dip⁹ in an extracavity arrangement in a fashion reminiscent of the early Lamb-dip spectroscopy experiments in which “probe” and “saturating” waves both saturate. Although their work is not complicated by standing waves, they still do not obtain the simplicity of a linear probe.

This polarized-field saturation spectroscopy is the fourth saturation spectroscopy, corresponding to the four kinds of mode interactions discussed in Sec. 4 of Ref. 15. One other is also new¹³ (grating-dip spectroscopy). The remaining two are well known as Lamb-dip (and related spectral) spectroscopy and the three-level spectroscopy discussed, for example, in Ref. 1.

It is a great pleasure to thank F. Keilmann and P. Toschek for stimulating discussions on this and related work.

*On sabbatical leave from the Optical Sciences Center, The University of Arizona. Work supported in part by a Senior U. S. Scientist Award (administered by the Alexander von Humboldt Stiftung) and in part by the

Space and Missile Systems Organization, Los Angeles.
¹³See, for example, reviews by V. P. Chebotayev, by J. L. Hall, and by V. S. Letokhov, in *High Resolution Laser Spectroscopy*, edited by K. Shimoda (Springer,

- Heidelberg, 1976).
- ²F. Keilmann (unpublished); M. Sargent (unpublished).
- ³J. L. Hall, Ref. 1.
- ⁴Polarization dependences have been considered in a three-level scheme, somewhat more complicated than the two-level approach here, by N. Skribanowitz, M. J. Kelley, and M. S. Feld, Phys. Rev. A 6, 2302 (1972).
- ⁵For a review, see Chap. 12 of M. Sargent III, M. O. Scully, and W. E. Lamb, Jr., *Laser Physics* (Addison-Wesley, Reading, Mass., 1974).
- ⁶R. L. Fork, L. E. Hargrove, and M. A. Pollack, Phys. Rev. Lett. 12, 705 (1964). For theory, see Ref. 9.
- ⁷M. Dumont, J. Phys. (Paris) 33, 971 (1972).
- ⁸M. A. Pollack and W. J. Tomlinson, Appl. Phys. Lett. 12, 173 (1968).
- ⁹M. Sargent III, W. E. Lamb, Jr., and R. L. Fork, Phys. Rev. 164, 436 (1967); 164, 450 (1967).
- ¹⁰D. R. Hanson and M. Sargent III, Phys. Rev. A 9, 466 (1974); and unpublished.
- ¹¹A. Dienes, Phys. Rev. 174, 400 (1968); 174, 414 (1968).
- ¹²Corresponding dependences in laser operation were first noted by C. V. Heer and R. D. Graft, Phys. Rev. 140, A1088 (1965).
- ¹³M. Sargent III, Appl. Phys. 9, 127 (1976).
- ¹⁴M. Gorlicki and M. Dumont, Opt. Commun. 11, 166 (1974).
- ¹⁵M. Sargent III, in *Applications of Lasers to Atomic and Molecular Physics*, edited by R. Balian and S. Haroche (North-Holland, Amsterdam, 1976).